

Fractals

Ruaidhrí Campion
JS Theoretical Physics
19333850

29th November 2021

CONTENTS

1 Abstract	2
2 Introduction	2
2.1 Fractal Properties	2
2.2 Mass Dimension Method	2
2.3 Box Counting Method	3
2.4 Electrodeposition Fractals	3
3 Method	4
4 Results & Discussion	5
5 Error Calculations	9
6 Conclusion	10
7 References	10

1 ABSTRACT

In this laboratory, the fractal shape and dimension of an electrodeposition of zinc sulfate was examined for varying molar concentration and applied voltage of a solution zinc sulfate monohydrate in deionised water. A correlation between fractal shape and combination of concentration and voltage was found by plotting a concentration-voltage phase diagram, and analysing the shapes of the different growths. A relationship between the fractal dimension of a growth and the molar concentration of the solution was identified, but the same was not true for fractal dimension and voltage. Finally, the reliability of different dimension calculating algorithms was also tested.

2 INTRODUCTION

2.1 FRACTAL PROPERTIES

In 1975, Benoit Mandelbrot coined the term “fractal”.¹ Throughout history, however, mathematicians have discovered many different fractal patterns, such as the Weierstrass function,² the Cantor set,³ or the Koch snowflake.⁴ Fractals have two main properties in common: self-similarity and non-integer fractal dimension.

The concept of self-similarity, or scale-independence, is straightforward; a self-similar pattern contains regions that are similar to or exactly the same as the entire pattern. Perhaps the most basic self-similar pattern is a line; no matter what scale a line is viewed over, its shape remains the same, i.e. given an image of a line, it is not possible to deduce what the scale of the image is.

Fractal dimension, however, is not so trivial. Although there are many (not always equivalent) ways to calculate the dimension of a fractal, it is typically used to describe a pattern’s “irregularity and breakage”,¹ or how detailed a pattern becomes once it is viewed over smaller scales. Unlike topological dimension, fractal dimension need not always be an integer; for example, the dimension of a line is 1, however the fractal dimension of the Cantor set, obtained by removing segments from a line, is $\frac{\log 2}{\log 3} \approx 0.63$.⁵ In this laboratory, two main methods of calculating fractal dimension are employed: the mass dimension method and the box counting method.

2.2 MASS DIMENSION METHOD

The mass dimension method employs a circle of varying radius centred at a given point. For a given radius r , the number of points N of the fractal (i.e. the amount of “mass”) within a circle of radius r is counted. By repeating this for a range of radii, the dependence of the number of points on the radius of the circle $N(r)$ can be obtained. The fractal dimension using this method is defined as

$$d_{\text{mass}} = \frac{\log N(r)}{\log r}. \quad (1)$$

For example, consider a point P on a square of side length a full of points. For a given radius $r < a$, the “mass” within a circle of radius r is proportional to r^2 , and thus the mass dimension d_{mass} is simply 2, the dimension of the plane. If a different shape was considered, however, the calculated dimension would not simply be the dimension of the space it lies in.

2.3 BOX COUNTING METHOD

The box counting method is the most intuitive of the two methods used in this laboratory. A grid containing boxes of side length l is laid across the fractal, and the number of boxes N containing any portion of the fractal is counted. By repeating this for a range of lengths, the dependence of the number of boxes containing the fractal $N(l)$ can be obtained. The fractal dimension using this method is defined as

$$d_{\text{box}} = \frac{\log N(l)}{\log \frac{1}{l}}. \quad (2)$$

Consider the same example as before, i.e. a square of side length a full of points. For $l = a, \frac{a}{2}, \frac{a}{3}, \frac{a}{4}, \dots$, the number of boxes containing a point is $N = 1, 4, 9, 16, \dots$, and so $N(l)$ is proportional to the squared reciprocal of l , thus $d_{\text{box}} = 2$, as in the mass dimension method. Like before, the same result would not necessarily occur for a different fractal.

2.4 ELECTRODEPOSITION FRACTALS

In this laboratory, “perfect” or “real” fractals were not considered. Instead, the behaviour of electrodeposits of zinc sulfate monohydrate (ZnSO_4) was examined. When a solution of ZnSO_4 is dissolved in deionised water over which a voltage is applied, crystals of zinc sulfate form in the solution, forming fractal-like shapes. Changing the molar concentration and voltage has an effect on the size, shape, and speed at which these clusters grow. This laboratory aimed to identify any correlation between these properties.

For electrodeposition fractals, such as those that will be formed in this laboratory, there exist four main shapes: diffusion-limited aggregation (DLA), dense radial, dendritic, and stringy. Examples of these fractal shapes can be seen in Figure 1.

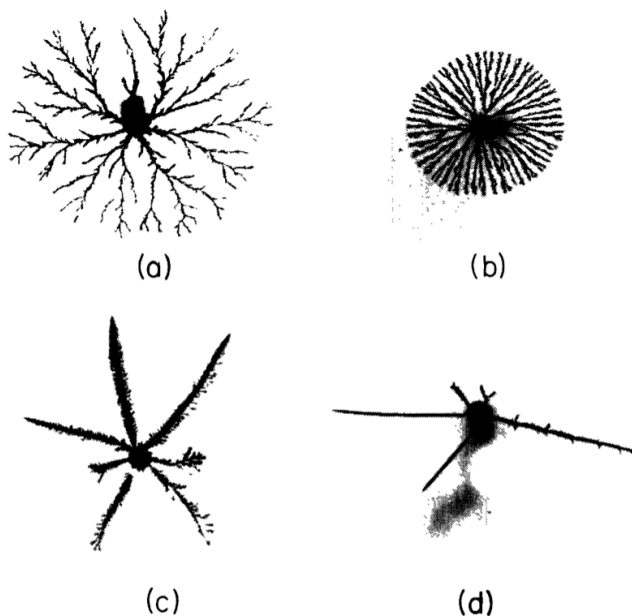


Figure 1: Different types of fractal shapes. (a) diffusion-limited aggregation, (b) dense radial, (c) dendritic, (d) stringy.⁶

3 METHOD

1. Dissolve an amount of zinc sulfate monohydrate (ZnSO_4) in deionised water corresponding to 1 molar solution (1 M).
2. Pour a portion of this solution into a sealed container, and dilute the remaining solution to obtain a lower concentration solution.
3. Repeat step 2 until several solutions of varying concentrations have been obtained.
4. Place several drops of a solution between perspex plates in order to create a thin film. With a zinc ring anode wedged between the plates and a graphite cathode placed through a hole in the centre of the top plate, apply a voltage to the system, turning off the voltage source once the zinc deposit is large enough, ensuring it does not touch the anode.
5. Place the perspex plate set-up underneath the provided CCD camera. Adjust the camera and lightbox settings until a clear image of the growth can be taken. Take a photograph of the growth and save it.
6. Using the ImageJ software, invert the colour scheme of the captured photograph so that the growth is white and its surroundings black. If the image contains the ring anode, crop the image accordingly. Record the centre position of the fractal, and save the image as a .bmp file.
7. Using the Benoit software, calculate the fractal dimension of the growth using both the mass dimension and box counting methods.
8. Repeat steps 4 - 7 for various concentration and voltage combinations.

4 RESULTS & DISCUSSION

The following photographs of each growth were taken:

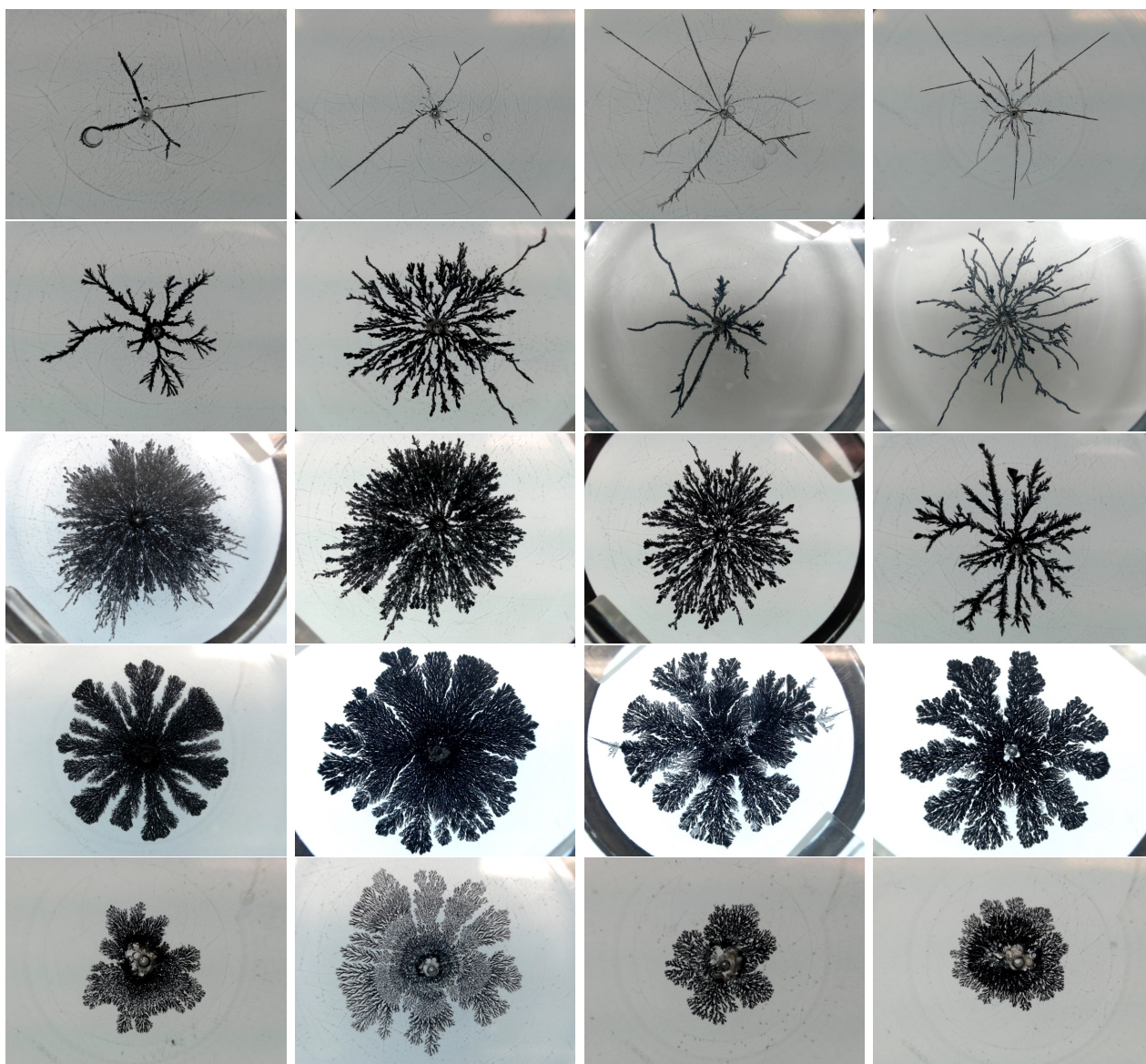


Figure 2: Photographs of zinc growth for varying molar concentration and voltage. From top to bottom, the molar concentration (in M) for each row is 1.0 ± 0.1 , 0.28 ± 0.05 , 0.11 ± 0.02 , 0.031 ± 0.008 , and 0.010 ± 0.003 . From left to right, the voltage (in V) for each column is 5.0 ± 0.1 , 10.0 ± 0.1 , 15.0 ± 0.1 , and 20.0 ± 0.1 .

The following fractal dimensions and fractal shape for each concentration and voltage combination was obtained:

Concentration, M	Voltage, V	Mass dimension	Box counting dimension	Fractal shape
1.0 ± 0.1	5.0 ± 0.1	1.3 ± 0.6	1.23 ± 0.05	stringy/dendrite
	10.0 ± 0.1	1.4 ± 0.5	1.29 ± 0.07	stringy
	15.0 ± 0.1	1.3 ± 0.4	1.28 ± 0.03	stringy
	20.0 ± 0.1	1.3 ± 0.5	1.352 ± 0.003	stringy
0.28 ± 0.05	5.0 ± 0.1	1.6 ± 0.3	1.57 ± 0.01	dendrite
	10.0 ± 0.1	1.76 ± 0.09	1.73 ± 0.01	dendrite
	15.0 ± 0.1	1.79 ± 0.07	1.707 ± 0.005	dendrite/stringy
	20.0 ± 0.1	1.7 ± 0.2	1.618 ± 0.004	dendrite/stringy
0.11 ± 0.02	5.0 ± 0.1	1.7 ± 0.2	1.668 ± 0.007	dense radial
	10.0 ± 0.1	1.90 ± 0.02	1.801 ± 0.005	dense radial/dendrite
	15.0 ± 0.1	1.93 ± 0.03	1.83 ± 0.01	dendrite/dense radial
	20.0 ± 0.1	2.04 ± 0.07	1.828 ± 0.006	dendrite
0.031 ± 0.008	5.0 ± 0.1	1.88 ± 0.05	1.84 ± 0.02	dense radial/DLA
	10.0 ± 0.1	1.922 ± 0.008	1.870 ± 0.009	dense radial
	15.0 ± 0.1	1.92 ± 0.02	1.847 ± 0.006	dense radial
	20.0 ± 0.1	2.02 ± 0.06	1.834 ± 0.008	dense radial
0.010 ± 0.003	5.0 ± 0.1	1.9 ± 0.4	1.79 ± 0.04	DLA
	10.0 ± 0.1	1.8 ± 0.2	1.80 ± 0.02	DLA
	15.0 ± 0.1	2.0 ± 0.7	1.80 ± 0.05	DLA
	20.0 ± 0.1	1.88 ± 0.02	1.81 ± 0.02	DLA/dense radial

Figure 3: The fractal dimension using each method and corresponding shape for each combination of molar concentration and voltage.

As can be seen from this data, the accuracy of the fractal dimension differs greatly based on what method is used; the average uncertainty for the box counting dimension is 0.02, whereas the same for the mass dimension is 0.2.

A possible reason for the large difference in uncertainty is the fact that the mass dimension method has a physical upper bound to its algorithm; once the mass dimension algorithm reaches a radius larger than the given fractal, the number of points within the circle does not increase, and so the corresponding plot will no longer be linear. Attempting to make a linear fit to a non-linear curve will result in a large uncertainty. This is clearly noticeable when comparing the photographs of the growth; for fractals that take up most of the image, the maximum allowable radius will reach the edge of the photograph, and so the corresponding uncertainty will be quite low, i.e. 0.008 - 0.06 uncertainty for 0.031 ± 0.008 M. For fractals that take up a small portion of the image, the maximum allowable radius will be quite small, and so the corresponding uncertainty will be quite high, i.e. 0.4 - 0.6 uncertainty for 1.0 ± 0.1 M. The only similar limitation of the box counting method is the resolution of the image, which thus imposes a smallest mesh size of the method. This, however, is also a limitation of the mass dimension method, as the accuracy of the circle used in each iteration directly depends on the number of pixels available.

The box counting method used by the Benoit software, however, was not without its flaws. A calibration test for the box counting method was performed on pictures of a straight line in various orientations, a blank page, and a checkerboard pattern. Although the dimension of a straight line in various orientations (1.04 ± 0.05 , 1.00 ± 0.06 , 1.05 ± 0.08) and of a line

segment (0.87 ± 0.05) were as expected, the dimension of a blank page (1.01 ± 0.18) and of a checkerboard pattern (1.79 ± 0.04) were not 0 and 2, respectively, as would be expected.

Another note to be made from Figure 3 is the correlation between molar concentration and both fractal dimension and shape; a higher concentration corresponds to a lower fractal dimension and a dendritic or stringy shape, whereas a lower concentration corresponds to a higher fractal dimension and a DLA or dense radial shape. This correlation is more apparent in the following graphs:

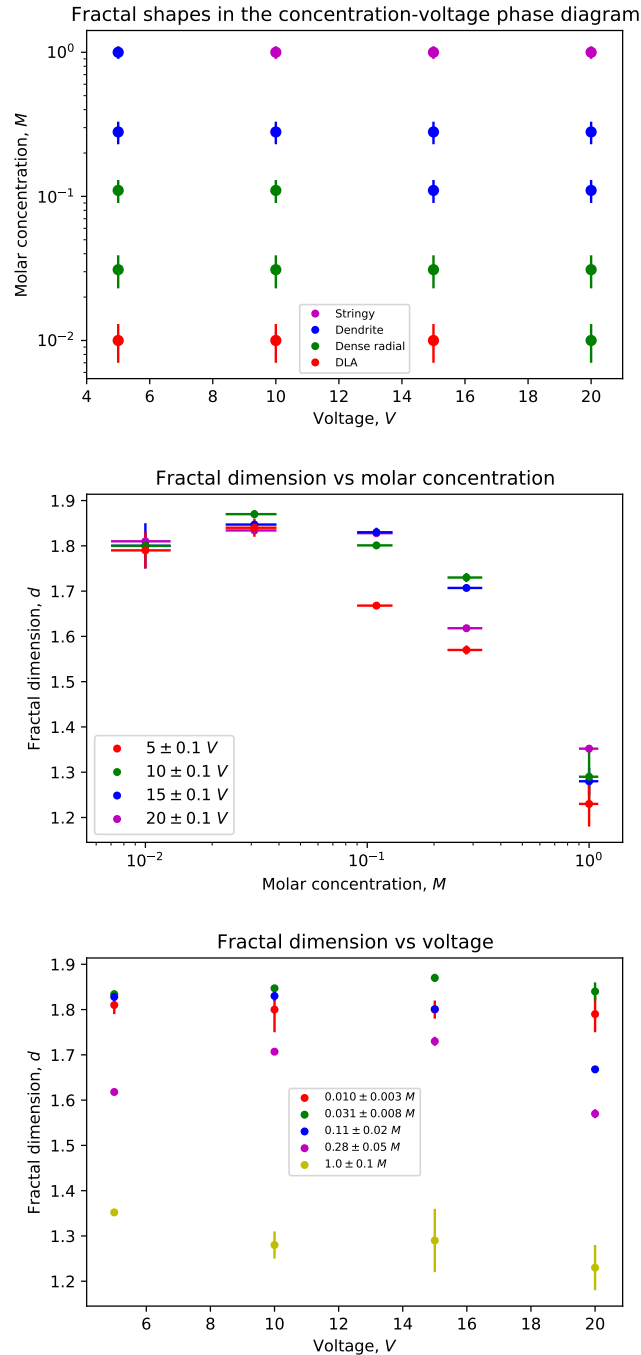


Figure 4: Graphs showing correlation between molar concentration, voltage, fractal shape, and fractal dimension. First graph: concentration-voltage phase space indicating fractal shapes. Second graph: plot of fractal dimension against molar concentration. Third graph: plot of fractal dimension vs voltage.

It can be seen from the first graph that the fractal shapes are separated in the phase diagram similarly to the graphs in Figure 5.

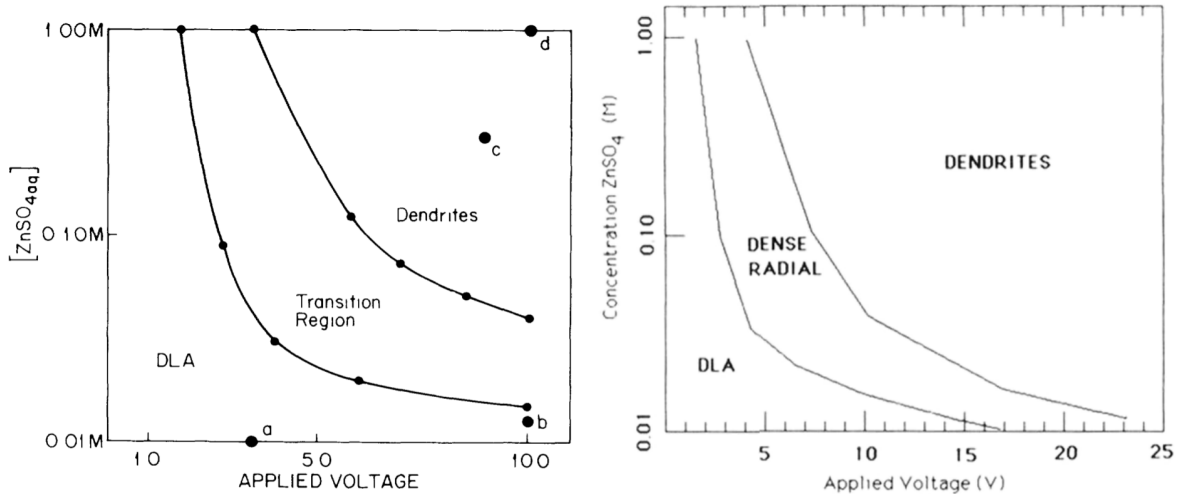


Figure 5: Phase diagrams experimentally obtained by Grier et al.^{6,7}

It can also be seen from the second and third graphs in Figure 4 that the fractal dimension has little to no dependence on voltage, yet there is a non-trivial dependence on molar concentration; for each concentration the fractal dimension remains roughly constant as voltage varies, whereas for each voltage it reaches a maximum at approximately 0.03 M.

The fractal dimensions used in the second and third graphs of Figure 4 were those calculated using the box counting method, due to the relatively high uncertainty in the mass dimension method. The mass dimension method is also comparably unreliable due to the fact the centre of the fractal is an input, which can be another source of error. Below is a table of the fractal dimensions calculated for 1.0 ± 0.1 M, for varying choice of centre point:

Voltage, V	Centre point, (x, y)	Dimension
5.0 ± 0.1	(313,240)	1.3 ± 0.4
	(318,240)	1.3 ± 0.6
	(320,240)	1.4 ± 0.8
10.0 ± 0.1	(290,159)	1.4 ± 0.4
	(295,159)	1.4 ± 0.5
	(270,199)	2.4 ± 0.7
15.0 ± 0.1	(313,232)	1.3 ± 0.3
	(318,232)	1.3 ± 0.4
	(267,231)	2 ± 1
20.0 ± 0.1	(300,235)	1.3 ± 0.5
	(305,235)	1.3 ± 0.5
	(305,234)	1.3 ± 0.5

Figure 6: The fractal dimension calculated using the mass dimension method using various points as the centre of the fractal, for 1 M. For each voltage, the first point is a shift of 5 pixels from the determined centre, the second point is the determined centre, and the third point is the default centre, i.e. the centre of the image. The difference in dimension using the default centre for 10.0 ± 0.1 V and 15.0 ± 0.1 V arises from the fact that the centre of the image was not close to the determined centre.

From the above data, it can be seen that the uncertainty in the fractal dimension varies in a high proportion when the centre point is slightly changed. Given this, and the generally high uncertainty in the mass dimension method, considering only the box counting dimension for the graphs in Figure 4 was reasonable.

5 ERROR CALCULATIONS

The uncertainty in the voltage applied to the system was found to be 0.1 V due to the precision of the voltmeter. The uncertainties in the fractal dimension were taken as the standard deviation calculated from the plots using the Benoit software. The uncertainties in the molar concentration were calculated using Gauss's law of error propagation

$$f = f(x, y) \implies \Delta f = \sqrt{\left(\frac{\partial f}{\partial x} \Delta x\right)^2 + \left(\frac{\partial f}{\partial y} \Delta y\right)^2}. \quad (3)$$

For example, the solution after step 1 of the method corresponded to a mass M_1 of 17.98 ± 0.01 g of ZnSO_4 dissolved in a volume V_1 of 0.10 ± 0.01 L of deionised water. Using the concentration formula $C = \frac{M}{V}$, the concentration can be calculated as

$$\begin{aligned} C_1 &= \frac{M_1}{V_1} & \Delta C_1 &= \sqrt{\left(\frac{\partial C_1}{\partial M_1} \Delta M_1\right)^2 + \left(\frac{\partial C_1}{\partial V_1} \Delta V_1\right)^2} \\ &= \frac{17.98 \text{ g}}{0.10 \text{ L}} & &= \sqrt{\left(\frac{\Delta M_1}{V_1}\right)^2 + \left(-\frac{M_1 \Delta V_1}{V_1^2}\right)^2} \\ &= 179.8 \text{ g/L} & &= \sqrt{\left(\frac{0.01 \text{ g}}{0.10 \text{ L}}\right)^2 + \left(\frac{17.98 \text{ g} \cdot 0.01 \text{ L}}{(0.10 \text{ L})^2}\right)^2} \\ & & &\approx 17.98 \text{ g/L} \end{aligned}$$

Given that the molecular mass of ZnSO_4 is 179.45 u, 1 M corresponds to 179.45 g dissolved in 1 L, and so the concentration is $C_1 \approx 1.0 \pm 0.1$ M. After this was obtained, 0.025 ± 0.001 L of the solution was transferred to a sealed container for use in the experiment. Since the concentration of the remaining solution C_2 was unchanged, $C_2 = C_1$. The volume of the remaining solution V_2 was 0.075 ± 0.01 ; the uncertainty is the same as that of V_1 due to the relatively low uncertainty in the removed volume. The mass of zinc in the remaining solution was found as

$$\begin{aligned} M_2 &= C_2 V_2 & \Delta M_2 &= \sqrt{\left(\frac{\partial M_2}{\partial C_2} \Delta C_2\right)^2 + \left(\frac{\partial M_2}{\partial V_2} \Delta V_2\right)^2} \\ &= 179.8 \pm 17.98 \text{ g/L} \cdot 0.075 \pm 0.010 \text{ L} & &= \sqrt{(V_2 \Delta C_2)^2 + (C_2 \Delta V_2)^2} \\ &= 13.485 \text{ g} & &= \sqrt{(0.075 \text{ L} \cdot 17.98 \text{ g/L})^2 + (179.8 \text{ g/L} \cdot 0.01 \text{ L})^2} \\ & & &\approx 2.255 \text{ g} \end{aligned}$$

Thus the mass M_2 of ZnSO_4 remaining is 13.385 ± 2.255 g. Next, deionised water was added until the volume V_3 of the solution was 0.27 ± 0.01 L. The weight M_3 of ZnSO_4 remains

unchanged, i.e. $M_3 = M_2$. The concentration C_3 was found similarly to before as

$$\begin{aligned}
 C_3 &= \frac{M_3}{V_3} & \Delta C_3 &= \sqrt{\left(\frac{\Delta M_3}{V_3}\right)^2 + \left(-\frac{M_3 \Delta V_3}{V_3^2}\right)^2} \\
 &= \frac{13.485 \text{ g}}{0.27 \text{ L}} & &= \sqrt{\left(\frac{2.255 \text{ g}}{0.27 \text{ L}}\right)^2 + \left(\frac{13.485 \text{ g} \cdot 0.01 \text{ L}}{(0.27 \text{ L})^2}\right)^2} \\
 &= 49.9444 \text{ g/L} & &= 8.5531 \text{ g/L}
 \end{aligned}$$

Dividing C_3 by 179.45 g/L results in a molar solution of 0.28 ± 0.05 M. The remaining concentrations were calculated in a similar fashion.

6 CONCLUSION

As expected, varying the molar concentration and applied voltage of a solution of ZnSO_4 in water changed both the fractal dimension and shape of the resulting crystalline structure. Although altering the voltage for a constant molar concentration did not seem to change the fractal dimension much, the fractal dimension had a non-trivial dependence on molar concentration at constant voltage. A graph similar to those in Figure 5 was produced in this laboratory, and it was shown that the box counting method is more reliable than the mass dimension method for calculating fractal dimension.

7 REFERENCES

- 1: B Mandelbrot, *Les objets fractals: forme, hasard et dimension*, Flammarion, Paris, (1975).
- 2: K Weierstrass, "6 - Über continuirliche Functionen eines reellen Arguments, die für keinen Werth des letzteren einen bestimmten Differentialquotienten besitzen" in *Mathematische Werke*, Cambridge University Press, Cambridge, (1872, republished in 2013).
- 3: G Cantor, *Über unendliche, lineare Punktmannichfaltigkeiten*, *Mathematische Annalen*, **21**, 545–591, (1883).
- 4: H von Koch, *Sur une courbe continue sans tangente, obtenue par une construction géométrique élémentaire.*, *Arkiv för matematik, astronomi och fysik*, **1**, 681-702 (1904).
- 5: M Hassan, G Rodgers, *Models of fragmentation and stochastic fractals*, *Physics Letters A*, **208**, 95-98, (1995).
- 6: D Grier et al, *Morphology and Microstructure in Electrochemical Deposition of Zinc*, *Physics Review Letters*, **56**, 1264-1267, (1986).
- 7: D Grier et al, *Stability of the Dense Radial Morphology in Diffusive Pattern Formation*, *Physics Review Letters*, **59**, 2315-2318, (1987).